

Physical Processes of Interstellar Turbulence

Enrique Vázquez-Semadeni¹

¹Centro de Radioastronomía y Astrofísica, UNAM Campus Morelia, 58089 México. E-mail: e.vazquez@crya.unam.mx

Abstract This review discusses the role of radiative heating and cooling, as well as self-gravity, in shaping the nature of the turbulence in the interstellar medium (ISM) of our galaxy. The ability of the gas to radiatively cool, while simultaneously being immersed in a radiative heat bath, causes it to be much more compressible than if it were adiabatic, and, in some regimes of density and temperature, to become thermally unstable, and thus tend to spontaneously segregate into separate phases, one warm and diffuse, the other dense and cold. On the other hand, turbulence is an inherently mixing process, thus tending to replenish the density and temperature ranges that would be forbidden under thermal processes alone. The turbulence in the ionized ISM appears to be transonic (i.e, with Mach numbers $M_s \sim 1$), and thus to behave essentially incompressibly. However, in the neutral medium, thermal instability causes the sound speed of the gas to fluctuate by up to factors of ~ 30 , and thus the flow can be highly supersonic with respect to the dense, cold gas, although numerical simulations suggest that the supersonic velocity dispersion corresponds more to the ensemble of cold clumps than to the clumps' internal velocity dispersion. Finally, coherent large-scale compressions in the warm neutral medium (induced by, say, the passage of spiral arms or by supernova shock waves) can produce large, dense clouds that are affected by their own self-gravity, and begin to contract gravitationally. Because they are populated by large-amplitude density fluctuations, whose local free-fall times can be significantly smaller than that of the whole cloud, the fluctuations terminate their collapse earlier, giving rise to a regime of hierarchical gravitational fragmentation, with small-scale collapses occurring within larger-scale ones. Thus, the “turbulence” in the cold, dense clouds may be dominated by a gravitationally contracting component at all scales.

1 Introduction

Our galaxy, the Milky Way (or simply, the Galaxy) is a flattened conglomerate of stars, gas, dust, and other debris, such as planets, meteorites, etc., with a total mass $\sim 10^{12} M_{\odot}$, where $M_{\odot} = 2 \times 10^{33}$ g is the mass of the Sun. Most of this mass is believed to be in a roughly spherical dark matter halo, while $\sim 10^{11} M_{\odot}$ are in stars, and $\sim 10^{10} M_{\odot}$ are contained in the gaseous component, mostly confined to the Galactic disk (Cox, 2000).

The gaseous component may be in either ionized, neutral atomic or neutral molecular forms, spanning a huge range of densities and temperatures, from the so-called hot ionized medium (HIM), with densities $n \sim 10^{-2} \text{ cm}^{-3}$ and temperatures $T \sim 10^6$ K, through the warm ionized and neutral (atomic) media (WIM and WNM, respectively), with $n \sim 0.3 \text{ cm}^{-3}$ and $T \sim 10^4$ K and the cold neutral (atomic) medium (CNM, $n \sim 30 \text{ cm}^{-3}$, $T \sim 100$ K, to the *giant molecular clouds* (GMCs, $n \gtrsim 100 \text{ cm}^{-3}$ and $T \sim 10\text{--}20$ K. GMCs can span several tens of parsecs across, and, in turn, have plenty of substructure, which are commonly referred to as *clouds* ($n \sim 10^3 \text{ cm}^{-3}$, size scales L of a few parsecs), *clumps* ($n \sim 10^4 \text{ cm}^{-3}$, $L \sim 1$ pc), and *cores* ($n \gtrsim 10^5 \text{ cm}^{-3}$, $L \sim 0.1$ pc), although the temperature of all molecular gas is remarkably uniform, $\sim 10\text{--}30$ K (e.g., Ferrière, 2001).

The gaseous component, along with the dust, a cosmic-ray background, and a magnetic field of mean intensity of a few μG constitute what we know as the *interstellar medium* (ISM). This medium is in most cases well described by the fluid approximation (Shu, 1992, Ch. 1). Moreover, the ISM is most certainly turbulent, as typical Reynolds numbers in it are very large. For example, in the cold ISM, $Re \sim 10^5\text{--}10^7$ (Elmegreen & Scalo, 2004, Sec. 4.1). This is mostly due to the very large spatial scales involved in interstellar flows. Because the ISM's temperature varies so much from one type of region to another, so does the sound speed, and the flow is often super- or trans-sonic (e.g., Heiles & Troland, 2003; Elmegreen & Scalo, 2004, and references therein). This implies that the flow is significantly compressible, inducing significant density fluctuations (Sec. 3.2).

In addition to being turbulent, the ISM is subject to a number of additional physical processes, such as gravitational forces exerted by the stellar and dark matter components as well as by the ISM itself (i.e., by its *self-gravity*), magnetic fields, cooling by radiative microscopic processes, and radiative heating due both to nearby stellar sources as well as to diffuse background radiative fields. All of this adds up to make the ISM an extremely complex and dynamical medium.

Finally, the self-gravity of the gas causes local (i.e., spatially intermittent) gravitational collapse events, in which a certain gas parcel within a molecular cloud goes out of equilibrium between its self-gravity and all other forces that oppose it, undergoing an implosion that leads the gas density to increase by many orders of magnitude, and whose end product is a star or a group (“cluster”) of stars.

In this review, we focus on the interaction between turbulence and the effects of radiative heating and cooling, which effectively enhance the compressibility of the flow, and have a direct effect on the star formation process. The plan of the paper is as follows: in Sec. 2 we first review the effects that the net heating and cooling have

on the effective equation of state of the flow and, in the case of thermally unstable flows, on its tendency to spontaneously segregate in distinct phases. Next, in Sec. 3 we discuss a few basic notions about turbulence and the turbulent production of density fluctuations in the compressible case, to then discuss, in Sec. 4, the interplay between turbulence and the heating and cooling. In Sec. 5, we discuss the likely nature of turbulence in the diffuse (warm and hot) parts of the ISM, while in Sec. 6 we do the same for the dense, cold atomic and molecular clouds. We conclude in Sec. 7 with a summary and some final remarks. Due to space limitations, we do not discuss magnetic fields, although we refer the interested reader to the reviews by Vázquez-Semadeni et al. (2000b), Cho et al. (2003), Elmegreen & Scalo (2004), and McKee & Ostriker (2007).

2 ISM Thermodynamics: Thermal Instability

The ISM extends essentially over the entire disk of the Galaxy and, when considering a certain subregion of it, such as a cloud or cloud complex, it is necessary to realize that any such subregion constitutes an open system, whose interactions with its environment need to be taken into account. A fundamental form of interaction with the surroundings, besides dynamical interactions, is through the exchange of heat. Indeed, the ISM is permeated by a radiation field, due to the combined shine of the stars in the disk. Moreover, a bath of relativistic charged particles, mostly protons, known as *cosmic rays*, also exists in the ISM. These are believed to be accelerated in strong shocks produced by supernova explosions (Blandford & Eichler, 1987). Both UV radiation and cosmic rays provide heating and ionization sources for the ISM at large (see, e.g., Dalgarno & McCray, 1972; Wolfire et al., 1995). Finally, violent events, such as supernova explosions, can locally heat their surroundings to very high temperatures, causing local bubbles of hot, million-degree ionized gas.

On the other hand, the ISM can cool by emission from ions, atoms and molecules, and by thermal emission from dust grains (Dalgarno & McCray, 1972; Sutherland & Dopita, 1993; Wolfire et al., 1995). The balance between these radiative heating and cooling radiative processes, along with the heat due to mechanical work and thermal conductivity, determine the thermodynamic properties of the ISM. These properties will be the focus of the present section, rather than the detailed microphysical processes that mediate the radiative transfer, about which there exist plenty of excellent books and reviews (e.g., Dalgarno & McCray, 1972; Sutherland & Dopita, 1993; Osterbrock & Ferland, 2006).

Globally, and as a first approximation, the ISM is roughly isobaric, as illustrated in the left panel of Fig. 1. As can be seen there, most types of regions, either dilute or dense, lie within an order of magnitude from a thermal pressure $P \sim 3000 \text{ K cm}^{-3}$.¹ The largest deviations from this pressure uniformity are found in HII regions, which are the ionized regions around massive stars due to the star's UV radiation, and

¹ It is customary in Astrophysics to express pressure in units of $[\text{K cm}^{-3}]$. Strictly speaking, this corresponds to P/k , where k is the Boltzmann constant.

molecular clouds, which, as we shall see in Sec. 6, are probably pressurized by gravitational compression.

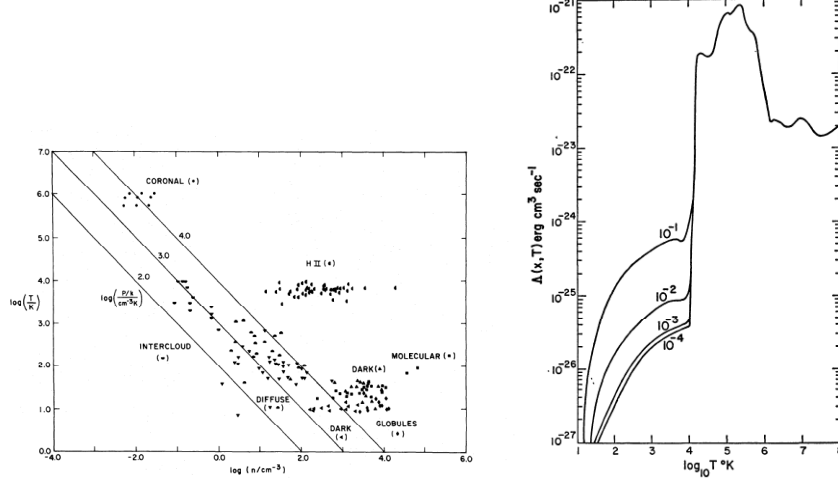


Fig. 1 *Left*: Thermal pressure in various types of interstellar regions. The points labeled *coronal* correspond essentially to what is referred to as the HIM in the text; *intercloud* regions refer to the WIM and WNM; *diffuse* to CNM clouds, and *dark*, *globule molecular* to molecular gas. From Myers (1978). *Right*: Temperature dependence of the cooling function. The labels indicate values of the ionization fraction (per number) of the gas. From Dalgarno & McCray (1972).

The peculiar thermodynamic behavior of the ISM is due to the functional forms of the radiative heating and cooling functions acting on it, which depend on the density, temperature, and chemical composition of the gas. The right panel of Fig. 1 shows the temperature dependence of the cooling function Λ (Dalgarno & McCray, 1972).

To understand the effect of the functional form of the radiative heating and cooling functions on the net behavior of the gas, let us write the conservation equation for the internal energy per unit mass, e . We have (e.g., Shu, 1992)

$$\frac{\partial e}{\partial t} + \mathbf{u} \cdot \nabla e = -(\gamma - 1)e \nabla \cdot \mathbf{u} + \Gamma - n\Lambda, \quad (1)$$

where we have neglected thermal conduction and heating by magnetic reconnection. In eq. (1), \mathbf{u} is the velocity vector, γ is the ratio of specific heats, Γ is the heating rate per unit mass, $n = \rho/\mu m_H$ is the number density, with μ the mean particle mass and m_H the hydrogen atom's mass. Note that $n\Lambda$ is the cooling rate per unit mass. The first term on the right hand side is the $P dV$ work per unit mass.

In the simplest possible case, that of a hydrostatic ($\mathbf{u} = 0$) and steady ($\partial/\partial t = 0$) state, eq. (1) reduces to the condition of *thermal equilibrium*,

$$\Gamma(\rho, T) = n\Lambda(\rho, T), \quad (2)$$

where we have denoted explicitly the dependence of Γ and Λ on the density and temperature, and neglected the dependence on chemical composition.

Let us now assume we have a gas parcel in thermal and hydrostatic equilibrium, at a temperature somewhere in the range where the slope of Λ with respect to T is negative (i.e., $(\partial\Lambda/\partial T)_\rho < 0$), $10^{5.5} \lesssim T \lesssim 10^6$ K (see the right panel of Fig. 1). If we then consider a small isochoric (i.e., at constant density) increase in T of this fluid parcel, we see that Λ decreases. Because we had started from thermal equilibrium, a drop in Λ implies that now $\Gamma > n\Lambda$, a condition that increases the parcel's temperature even further, causing a runaway to higher temperatures, until the fluid parcel exits the temperature range where $(\partial\Lambda/\partial T)_\rho < 0$, at $T \gtrsim 10^6$ K. This behavior is known as *thermal instability* (TI), and the condition $(\partial\Lambda/\partial T)_\rho < 0$ is known as the *isochoric criterion* for TI (Field 1965; see also the review by Vázquez-Semadeni et al. 2003).

Another, less stringent condition for the development of TI is the so-called *isobaric criterion*. This can be most easily understood as follows. Note that eq. (2) provides a relation between the density and temperature of the medium. This can be inserted in the equation of state for the gas,² allowing the elimination of the temperature from it and writing a *barotropic* equation of the form $P_{\text{eq}} = P_{\text{eq}}(\rho)$, where P_{eq} is the thermal pressure under conditions of thermal equilibrium, and is a function of the density only. Figure 2 shows the resulting density dependence of P_{eq} for the atomic medium under “standard” conditions (Wolfire et al., 1995). The region above the graph of $P_{\text{eq}}(n)$ corresponds to $n\Lambda > \Gamma$, and therefore to net cooling. Conversely, the area under the curve corresponds to net heating, $n\Lambda < \Gamma$. From this figure, we observe that the slope of the graph of P_{eq} vs. ρ is *negative* for densities in the range $0.6 \lesssim n \lesssim 5 \text{ cm}^{-3}$ (i.e., $-0.2 \lesssim \log_{10}(n/\text{cm}^{-3}) \lesssim 0.7$).

Let us now consider a fluid parcel in this density range, and apply to it a small, quasi-static compression (i.e., volume reduction) to it, increasing its density. This displaces the parcel to the region above the thermal equilibrium curve, where net cooling occurs. Because the compression is quasi-static, the parcel has time to cool under the effect of the net cooling, which causes its pressure to decrease as it attempts to return to the thermal equilibrium curve. But thus it is now at a lower pressure than its surroundings, which then continue to further compress the parcel, and runaway compression sets in, until the parcel exits the regime where $dP_{\text{eq}}/dn < 0$. The density range where this condition is met is called the *unstable range*.

Thus, if the mean density of the medium is in the unstable range, this mode of TI tends to cause the medium to spontaneously segregate into a cold, dense phase and a warm, diffuse one (Field et al., 1969). That is indeed the case of the ISM in the Galactic midplane in the Solar neighborhood, a fact which led Field et al. (1969) to propose the so-called *two-phase model* of the ISM: assuming dynamical and thermal equilibrium, the atomic ISM would consist of small dense, cold clumps (the CNM), immersed in a warm, diffuse background (the WNM). The clumps are expected to

² Given the low densities of the ISM, it is a good approximation to use the ideal gas equation of state.

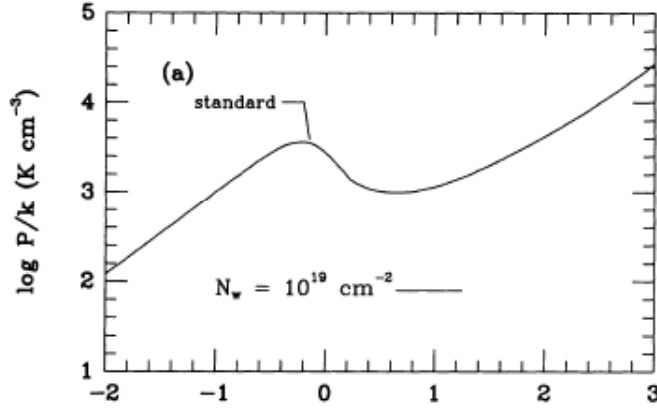


Fig. 2 Thermal-equilibrium pressure P_{eq} as a function of number density for “standard” conditions of metallicity and background UV radiation for the atomic medium. The horizontal axis gives $\log_{10}(n/\text{cm}^3)$. From Wolfire et al. (1995).

be small because the fastest growing mode of the instability occurs at vanishingly small scales in the absence of thermal conductivity, or at scales ~ 0.1 pc for the estimated thermal conductivity of the ISM (see, e.g., Audit & Hennebelle, 2005). Note that the isochoric criterion for TI implies that the isobaric one is satisfied, but not the other way around. Technical and mathematical details, as well as other modes of TI, can be found in the original paper by Field (1965), and in the reviews by Meerson (1996) and by Vázquez-Semadeni et al. (2003).

It is important to note that, even if the medium is *not* thermally unstable, the balance between heating and cooling implies a certain functional dependence of $P_{\text{eq}}(\rho)$, which is often approximated by a *polytropic* law of the form $P_{\text{eq}} \propto \rho^{\gamma_e}$ (e.g., Elmegreen, 1991; Vázquez-Semadeni et al., 1996), where it should be noted that γ_e , which we refer to as the *effective polytropic exponent*, is *not* the ratio of specific heats for the gas in this case, but rather a free parameter that depends on the functional forms of Λ and Γ . The isobaric mode of TI corresponds to $\gamma_e < 0$.

3 Compressible Turbulence

3.1 Equations

In the previous section we have discussed thermal aspects of the ISM, whose main dynamical effect is the segregation of the medium into the cold and warm phases. Let us now discuss dynamics. As was mentioned in Sec. 1, the ISM is in general highly turbulent, and therefore it is necessary to understand the interplay between

turbulence and the effects of the net cooling ($n\Lambda - \Gamma$), which affects the compressibility of the gas (Vázquez-Semadeni et al., 1996).

The dynamics of the ISM are governed by the fluid equations, which, neglecting magnetic fields, comprise eq. (1) and (e.g., Landau & Lifshitz, 1959; Shu, 1992)

$$\frac{\partial \rho}{\partial t} + \mathbf{u} \cdot \nabla \rho = -\rho \nabla \cdot \mathbf{u}, \quad (3)$$

$$\frac{\partial \mathbf{u}}{\partial t} + \mathbf{u} \cdot \nabla \mathbf{u} = -\frac{\nabla P}{\rho} - \nabla \phi + \nu \left[\nabla^2 \mathbf{u} + \frac{\nabla(\nabla \cdot \mathbf{u})}{3} \right], \quad (4)$$

$$\nabla^2 \phi = 4\pi G \rho, \quad (5)$$

where ϕ is the gravitational potential, and ν is the kinematic viscosity. Equation (3) represents mass conservation, and is also known as the *continuity equation*. Equation (4) is the momentum conservation, or *Navier-Stokes equation* per unit mass, with an additional source term representing the gravitational force $\nabla \phi / \rho$. In turn, the gravitational potential is given by *Poisson's equation*, eq. (5). Equations (1), (3), (4), and (5) are to be solved simultaneously, given some initial and boundary conditions.

A brief discussion of the various terms in eq. (4) is in order. The second term on the left is known as the *advective term*, and represents the transport of i -momentum by the j component of the velocity, where i and j represent any two components of the velocity. It is responsible for *mixing*. The pressure gradient term (first term on the right-hand side [RHS]) in general acts to counteract pressure, and therefore density, gradients across the flow. Finally, the term in the brackets on the RHS, the *viscous term*, being of a diffusive nature, tends to erase velocity gradients, thus tending to produce a uniform flow.

3.2 Reynolds and Mach numbers. Compressibility

Turbulence develops in a flow when the ratio of the advective term to the viscous term becomes very large. That is,

$$\frac{\mathcal{O}[\mathbf{u} \cdot \nabla \mathbf{u}]}{\mathcal{O}\left[\nu \left(\nabla^2 \mathbf{u} + \frac{\nabla(\nabla \cdot \mathbf{u})}{3}\right)\right]} \sim \frac{U^2}{L} \left[\nu \frac{U}{L^2} \right]^{-1} \sim \frac{UL}{\nu} \equiv Re \gg 1, \quad (6)$$

where Re is the *Reynolds number*, U and L are characteristic velocity and length scales for the flow, and \mathcal{O} denotes “order of magnitude”. This condition implies that the mixing action of the advective term overwhelms the velocity-smoothing action of the viscous term.

On the other hand, noting that the advective and pressure gradient terms contribute comparably to the production of density fluctuations, we can write

$$1 \sim \frac{\mathcal{O}(\mathbf{u} \cdot \nabla \mathbf{u})}{\mathcal{O}(\nabla P/\rho)} \sim \frac{U^2}{L} \left[\frac{\Delta P}{L\rho} \right]^{-1} \sim U^2 \left(\frac{c_s^2 \Delta \rho}{\rho} \right)^{-1} \equiv M_s^2 \left(\frac{\Delta \rho}{\rho} \right)^{-1}, \quad (7)$$

$$\Rightarrow \frac{\Delta \rho}{\rho} \sim M_s^2, \quad (8)$$

where $M_s \equiv U/c_s$ is the *sonic Mach number*, and we have made the approximation that $\Delta P/\Delta \rho \sim c_s^2$, where c_s is the sound speed. Equation (8) then implies that strong compressibility requires $M_s \gg 1$. Conversely, flows with $M_s \ll 1$ behave incompressibly, even if they are gaseous. Such is the case, for example, of the Earth's atmosphere. In the incompressible limit, $\rho = \text{cst.}$, and thus eq. (3) reduces to $\nabla \cdot \mathbf{u} = 0$.

Finally, a trivial, but often overlooked, fact is that, in order to produce a density enhancement in a certain region of the flow, the velocity at that point must have a negative divergence (i.e., a *convergence*), as indicated by the continuity equation, eq. (3). It is very frequent to encounter in the literature discussions of pre-existing density enhancements (“clumps”) in hydrostatic equilibrium. But it should be kept in mind that these can only exist in multi-phase media, where a dilute, warm phase can have the same pressure as a denser, but colder, clump. But even in this case, the *formation* of that clump must have initially involved the convergence of the flow towards the cloud, and the hydrostatic situation is applicable in the limit of very long times after the formation of the clump, when the convergence of the flow has subsided.

3.3 Production of Density Fluctuations

According to the previous discussion, a turbulent flow in which the velocity fluctuations are supersonic will naturally develop strong density fluctuations. Note, however, that the nature of turbulent density fluctuations in a single-phase medium (such as, for example, a regular isothermal or adiabatic flow) is very different from that of the cloudlets formed by TI (cf. Sec. 2). In a single-phase turbulent medium, turbulent density fluctuations must be transient, as a higher density generally conveys a higher pressure,³ and therefore the fluctuations must re-expand after the compression that produced them has subsided.

For astrophysical purposes it is important to determine the distribution of these fluctuations, as they may constitute, or at least provide the seeds for, what we normally refer to as “clouds” in the ISM. Because of the transient nature of turbulent density fluctuations in single-phase media, however, this distribution refers to a time-stationary population of fluctuations, although the fluctuations themselves will appear and disappear over times short compared to the time over which the distribution is considered.

³ An exception would be a so-called Burgers' flow, which is characterized by the absence of the pressure gradient term (Burgers, 1974).

The probability density distribution (PDF) of the density field in turbulent isothermal flows was first investigated numerically, finding that, in the isothermal case, it possesses a lognormal form (Vázquez-Semadeni, 1994). A theory for the emergence of this functional form was later proposed by Passot & Vázquez-Semadeni (1998), in which the production of density fluctuations was assumed to arise from a succession of compressive or expansive waves, each one acting on the value of the density left by the previous one. Because the medium contains a unique distribution of (compressible) velocity fluctuations, and because the density jumps in isothermal flow depend only on Mach number but not in the local density, the density fluctuations belong all to a unique distribution as well, yet each one can be considered independent of the others if the global time scales considered are much longer than the autocorrelation time of the velocity divergence (Blaisdell et al., 1993). Finally, because the density jumps are multiplicative in the density (cf. eq. 8), then they are additive in $s \equiv \ln \rho$. Under these conditions, the Central Limit Theorem can be invoked for the increments in s , implying that s will be normally distributed. In consequence, ρ will have a lognormal PDF.

In addition, Passot & Vázquez-Semadeni (1998) also argued that the variance of the density fluctuations should scale linearly with M_s , a fact that has been investigated further by various groups (Padoan et al., 1997; Passot & Vázquez-Semadeni, 1998; Federrath et al., 2008). In particular, using numerical simulations of compressible turbulence driven by either solenoidal (or “vortical”) or compressible (or “potential”) forces, the latter authors proposed that the variance of s is given by

$$\sigma_s = [\ln(1 + bM_s^2)] , \quad (9)$$

where b is a constant whose value depends on the nature of the forcing, taking the extreme values of $b = 1/3$ for purely solenoidal forcing, and $b = 1$ for purely compressible forcing. The lognormal density PDF for the one-dimensional simulations of Passot & Vázquez-Semadeni (1998), with its dependence on M_s , is illustrated in the *left panel* of Fig. 3.

Finally, Passot & Vázquez-Semadeni (1998, see also Padoan & Nordlund 1999) also investigated the case where the flow behaves as a polytrope with arbitrary values of γ_e , by noting that in this case the sound speed is not constant, but rather depends on the density as $c_s \propto \rho^{(\gamma_e-1)/2}$, implying that the local Mach number of a fluid parcel now depends on the local density besides its dependence on the value of the flow velocity. Introducing this dependence of M_s on ρ in the expression for the lognormal PDF, Passot & Vázquez-Semadeni (1998) concluded that the density PDF should develop a power-law tail, at high densities when $\gamma_e < 1$, and at low densities when $\gamma_e > 1$. This result was then confirmed by numerical simulations of polytropic turbulent flows (Fig. 3, *right panel*).

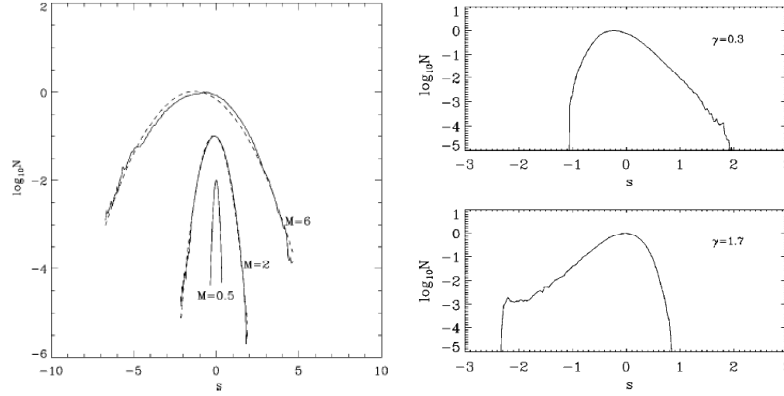


Fig. 3 *Left:* Lognormal density PDFs for isothermal one-dimensional simulations at various Mach numbers, indicated by the labels. The independent variable is $s \equiv \ln \rho$. *Right:* Density PDFs for polytropic cases, with effective polytropic exponent $\gamma_e = 0.3$ (*top*) and $\gamma_e = 1.7$ (*bottom*). From Passot & Vázquez-Semadeni (1998).

4 Turbulence and Thermodynamics

In the previous sections we have separately discussed two different kinds of physical processes operating in the ISM: radiative heating and cooling (to which we refer collectively as *net cooling*, $n\Lambda - \Gamma$), and compressible turbulence. However, since both operate simultaneously, it is important to understand how they interact with each other, especially because the mean density in the Solar neighborhood, $\langle n \rangle \sim 1 \text{ cm}^{-3}$, falls precisely in the thermally unstable range. This problem has been investigated numerically by various groups (e.g., Hennebelle & Péroult, 1999; Walder & Folini, 2000; Koyama & Inutsuka, 2000, 2002; Vázquez-Semadeni et al., 2000a, 2003, 2006; Gazol et al., 2001, 2005; Kritsuk & Norman, 2002; Sánchez-Salcedo et al., 2002; Piontek & Ostriker, 2004, 2005; Audit & Hennebelle, 2005; Heitsch et al., 2005; Hennebelle & Audit, 2007).

4.1 Density and Pressure Distributions in the ISM

The main parameter controlling the interaction between turbulence and net cooling is the ratio $\eta \equiv \tau_c / \tau_t$, where $\tau_c \approx e / (\mu m_H \rho \Lambda)$ is the cooling time and $\tau_t \approx L / U$ is the turbulent crossing time. The remaining symbols have been defined above. In the limit $\eta \gg 1$, the turbulent compressions evolve much more rapidly than they can cool, and therefore behave nearly adiabatically. Conversely, in the limit $\eta \ll 1$, the fluctuations cool down essentially instantaneously while the turbulent compression is evolving, and thus they tend to reach the thermal equilibrium

pressure P_{eq} as soon as they are produced⁴ (Elmegreen, 1991; Passot et al., 1995; Sánchez-Salcedo et al., 2002; Vázquez-Semadeni et al., 2003; Gazol et al., 2005). Because in a turbulent flow velocity fluctuations of a wide range of amplitudes and size scales are present, the resulting density fluctuations in general span the whole range between those limits, and the actual thermal pressure of a fluid parcel is not uniquely determined by its density, but rather depends on the details of the velocity fluctuation that produced it. This causes a scatter in the values of the pressure around the thermal-equilibrium value in the pressure-density diagram (Fig. 4, *left panel*), and also produces significant amounts of gas (up to nearly half of the total mass) with densities and temperatures in the classically forbidden thermally unstable range (Gazol et al., 2001; de Avillez & Breitschwerdt, 2005; Audit & Hennebelle, 2005; Mac Low et al., 2005), a result that has been encountered by various observational studies (e.g., Dickey et al., 1978; Heiles, 2001). In any case, the tendency of the gas to settle in the stable phases still shows up as a multimodality of the density PDF, which becomes less pronounced as the *rms* turbulent velocity increases (Fig. 4, *right panel*).

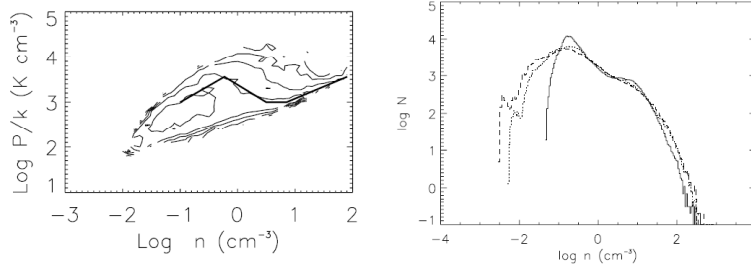


Fig. 4 *Left*: Two-dimensional histogram of the grid cells in the pressure-density diagram for a two-dimensional simulation of turbulence in the thermally-bistable atomic medium, with *rms* velocity dispersion of 9 km s^{-1} , a numerical box size of 100 pc, and the turbulent driving applied at a scale of 50 pc. *Right*: Density PDF in simulations like the one on the left panel, but with three different values of the *rms* velocity: 4.5 km s^{-1} (solid line), 9 km s^{-1} (dotted line), and 11.3 km s^{-1} (dashed line). From Gazol et al. (2005).

⁴ Note that it is often believed that fast cooling implies isothermality. However, this is an erroneous notion. While it is true that fast cooling is a necessary condition for isothermal behavior, the reverse implication does not hold. Fast cooling only implies an approach to the thermal equilibrium condition, but this need not be isothermal. The precise form of the effective equation of state depends on the details of the functional dependence of Λ and Γ on T and ρ .

4.2 The formation of dense, cold clouds

Another important consequence of the interaction of “turbulence” (or, more generally, large-scale coherent motions of any kind) and TI is that the former may *non-linearly* induce the latter. Indeed, Hennebelle & P  rault (1999, see also Koyama & Inutsuka 2000) showed that transonic (i.e., with $M_s \sim 1$) compressions in the WNM can compress the medium and bring it sufficiently far from thermal equilibrium that it can then undergo a phase transition to the CNM (Fig. 5, *left panel*). This process amounts then to producing a cloud with a density up to $100\times$ larger than that of the WNM by means of only moderate compressions. This is in stark contrast with the process of producing density fluctuations by pure supersonic compressions in, say, an isothermal medium, in which such density contrasts would require Mach numbers $M_s \sim 10$.

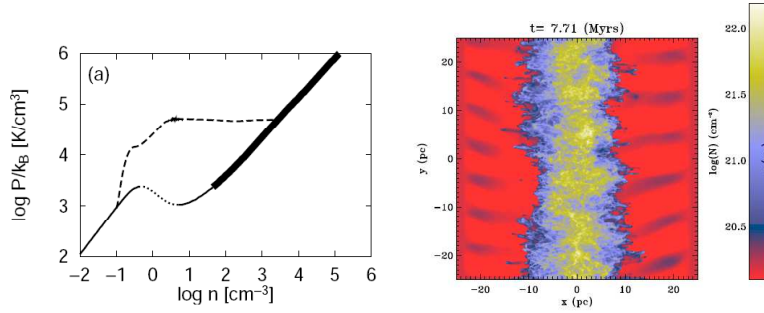


Fig. 5 *Left*: Evolutionary path (*dashed line*) in the P vs. ρ diagram of a fluid parcel initially in the WNM after suffering a transonic compression that nonlinearly triggers TI. The *solid* and *dotted lines* show the locus of $P_{eq}(\rho)$, the solid sections corresponding to linear stability and the dotted ones to linear instability. The solid section to the left of the dotted line corresponds to the WNM and the one at the right, to the CNM. The perturbed parcel evolves from left to right along the dashed line. From Koyama & Inutsuka (2000). *Right*: Projected (or *column*) density of a numerical simulation of the formation of a dense cloud formed by the convergence of two large-scale streams of WNM. The projection is along lines of sight perpendicular to the direction of compression. The cloud is seen to have become turbulent and highly fragmented. From Hennebelle et al. (2008).

Moreover, the cold clouds formed by this mechanism have typical sizes given by the size scale of the compressive wave in the transverse direction to the compression, thus avoiding the restriction of having the size scale of the fastest growing mode of TI, which is very small (~ 0.1 pc; cf. Sec. 2). The initial stages of this process may produce thin CNM sheets (V  zquez-Semadeni et al., 2006), which are in fact observed (Heiles & Troland, 2003). However, such sheets are quickly destabilized, apparently by a combination of nonlinear thin shell (NTSI; Vishniac, 1994), Kelvin-Helmholtz and Rayleigh-Taylor instabilities (Heitsch et al., 2005), fragmenting and becoming turbulent. This causes the clouds to become a complex mixture of cold and warm gas, where the cold gas is distributed in an intricate network of sheets,

filaments and clumps, possibly permeated by a dilute, warm background. An example of this kind of structure is shown in the *right panel* of Fig. 5.

5 Turbulence in the Ionized ISM

As discussed in the previous sections, the ionized and atomic components of the ISM consist of gas in a wide range of temperatures, from $T \sim 10^6$ K for the HIM, to $T \sim 40$ K for the CNM. In particular, Heiles & Troland (2003) report temperatures in the range $500 < T < 10^4$ K for the WNM, and in the range $10 < T < 200$ K for the CNM. The WIM is expected to have $T \sim 10^4$ K. Additionally, those same authors report column density-weighted *rms* velocity dispersions $\sigma_v \sim 11$ km s⁻¹ for the WNM, and $\sigma_v \sim 7$ km s⁻¹ for the CNM. Since the adiabatic sound speed is given by (e.g., Landau & Lifshitz, 1959)

$$c_s = \sqrt{\frac{\gamma k T}{\mu m_H}} = 10.4 \text{ km s}^{-1} \left(\frac{T}{10^4 \text{ K}} \right)^{1/2}, \quad (10)$$

it is clear that the warm, or *diffuse*, gas is transonic ($M_s \sim 1$), while the cold, or *dense*, gas is strongly supersonic ($3 \lesssim M_s \lesssim 20$). Indeed, collecting measurements of interstellar scintillation (fluctuations in amplitude and phase of radio waves caused by scattering in the ionized ISM) from a variety of observations, Armstrong et al. (1995) estimated the power spectrum of density fluctuations in the WIM, finding that it is consistent with a Kolmogorov spectrum, characteristic of incompressible turbulence (see, e.g., the reviews by Vázquez-Semadeni, 1999; Mac Low & Klessen, 2004; Elmegreen & Scalo, 2004), on scales $10^8 \lesssim L \lesssim 10^{15}$ cm.

More recently, using data from the Wisconsin H α Mapper Observatory, Chepurnov & Lazarian (2010) have been able to extend this result to scales $\sim 10^{19}$ cm, suggesting that the WIM behaves as an incompressible turbulent flow over size scales spanning more than 10 orders of magnitude. Although the WIM is ionized, and thus should be strongly coupled to the magnetic field, the turbulence then being magnetohydrodynamic (MHD), Kolmogorov scaling should still apply, according to the theory of incompressible MHD fluctuations (Goldreich & Sridhar, 1995). The likely sources of kinetic energy for these turbulent motions are stellar energy sources such as supernova explosions (see, e.g., Mac Low & Klessen, 2004).

6 “Turbulence” in the Atomic and Molecular ISM

6.1 *The atomic medium*

In contrast to the relatively clear-cut situation for the ionized ISM, the turbulence in the neutral (atomic and molecular) gas is more complicated, and is currently under strong debate. According to the discussion in Sec. 5, the temperatures in the atomic gas may span a continuous range from a few tens to several thousand degrees, and have velocity dispersions of $\sigma_v \sim 7\text{--}10 \text{ km s}^{-1}$, suggesting that it should range from mildly to strongly supersonic. But because the atomic gas is *thermally bistable* (i.e., has two stable thermodynamic phases separated by an unstable one; Sec. 2), and because transonic compressions in the WNM can nonlinearly induce TI and thus a phase transition to the CNM (Sec. 4.1), the neutral atomic medium is expected to consist of a complex mixture of gas spanning over two orders of magnitude in density. Early models (e.g., Field et al., 1969; McKee & Ostriker, 1977) proposed that the phases were completely separate, but the results reported in Sec. 4.1 suggest that significant amounts of gas exist as well in the unstable range, transitioning between the stable phases. Numerical simulations of such systems suggest that the velocity dispersion *within* the densest “clumps” is subsonic, but that the velocity dispersion of the clumps within the diffuse substrate is supersonic with respect to the clumps’ sound speed (although subsonic with respect to the warmest gas; Koyama & Inutsuka, 2002; Heitsch et al., 2005). Also, note that, contrary to earlier ideas (e.g. Kwan, 1979; Blitz & Shu, 1980), the clumps in the modern simulations actually form from *fragmentation* of large-scale clouds formed by large-scale compressive motions in the WNM, rather than the clouds forming from random collision and coagulation of the clumps. The complexity of this type of structure is illustrated in the *right panel* of Fig. 5.

6.2 *The Molecular Gas*

The discussion so far, involving mainly turbulence and thermodynamics, has referred to the ionized and atomic components of the ISM. However, molecular clouds (MCs) have long been known to be strongly self-gravitating (e.g., Goldreich & Kwan, 1974; Larson, 1981). In view of this, Goldreich & Kwan (1974) initially proposed that MCs should be in a state of gravitational collapse, and that the observed motions in MCs (as derived by the non-thermal linewidths of molecular lines) corresponded to this collapse. However, shortly thereafter, Zuckerman & Palmer (1974) argued against this possibility by noting that, if all the molecular gas in the Galaxy ($M_{\text{mol}} \sim 10^9 M_\odot$) were in free-fall, a simple estimate of the Galaxy’s star formation rate (SFR), given by $\text{SFR} \sim M_{\text{mol}}/\tau_{\text{ff}} \sim 200 M_\odot \text{ yr}^{-1}$, where $\tau_{\text{ff}} = \sqrt{3\pi/32G\rho}$ is the free-fall time, would exceed the observed rate of $\sim 3 M_\odot \text{ yr}^{-1}$ by roughly two orders of magnitude. This prompted the suggestion (Zuckerman & Evans, 1974) that

the non-thermal motions in MCs corresponded instead to small-scale (in comparison to the clouds' sizes) random turbulent motions. The need for these motions to be confined to small scales arose from the need of the turbulent (*ram*) pressure to provide an isotropic pressure that could counteract the clouds' self-gravity at large, maintaining them in near virial equilibrium (Larson, 1981). Because turbulence is known to be a dissipative phenomenon (e.g., Landau & Lifshitz, 1959), research then focused on finding suitable sources for driving the turbulence and avoiding rapid dissipation. The main driving source was considered to be energy injection from stars (e.g., Norman & Silk, 1980; McKee, 1989; Mac Low & Klessen, 2004), and reduction of dissipation was proposed to be accomplished by having the turbulence being MHD, and consisting mostly of Alfvén waves, which do not dissipate as rapidly (e.g., Shu et al., 1987).

However, in the last decade several results have challenged the turbulent pressure-support scenario: 1) Turbulence is known to be characterized by having the largest-velocities occur at the largest scales, and MCs are no exception, exhibiting scaling relations between velocity dispersion and size suggesting that the largest dispersions tend to occur at the largest scales (Larson, 1981; Heyer & Brunt, 2004; Brunt et al., 2009, Fig. 6, *left and middle panels*). This is inconsistent with the small-scale requirement for turbulent support. 2) It was shown by several groups that MHD turbulence dissipates just as rapidly as hydrodynamic turbulence (Mac Low et al., 1998; Stone et al., 1998; Padoan & Nordlund, 1999), dismissing the notion of reduced dissipation in “Alfvén-wave turbulence”, and thus making the presence of strong driving sources for the turbulence an absolute necessity. 3) Clouds with very different contributions from various turbulence-driving mechanisms, including those with little or no star formation activity, such as the so-called *Maddalena's cloud*, show similar turbulence characteristics (Williams et al., 1994; Schneider et al., 2011), suggesting that stellar energy injection is not the main source of turbulence in MCs.

Moreover, simulations of dense cloud formation have shown that, once a large cold CNM cloud forms out of a collision of WNM streams, it quickly acquires a large enough mass that it can begin to collapse gravitationally (Vázquez-Semadeni et al., 2007, 2010, 2011; Heitsch et al., 2008a,b). The enhancement in its column density promotes the formation of molecular hydrogen (H_2) (Hartmann et al., 2001; Bergin et al., 2004; Heitsch & Hartmann, 2008). Thus, it appears that the formation of a *molecular* cloud may require previous gravitational contraction (see also McKee, 1989). In addition, according to the discussion in Secs. 4.2 and 6.1, the CNM clouds formed by converging WNM flows should be born turbulent and clumpy. The turbulent nature of the clouds further promotes the formation of molecular hydrogen (Glover & Mac Low, 2007). The simulations by (Vázquez-Semadeni et al., 2007, 2010, 2011) show that the nonlinear, turbulent density fluctuations can begin to collapse *before* the global collapse of the cloud is completed (Fig. 6, *right panel*), both because their densities are large enough that their free-fall time is significantly shorter than that of the whole cloud, and because the free-fall time of a flattened or elongated cloud may be much larger than that of an approximately isotropic clump within it of the same volume density (Toalá et al., 2012). However, the turbulent velocities initially induced in the clouds by the con-

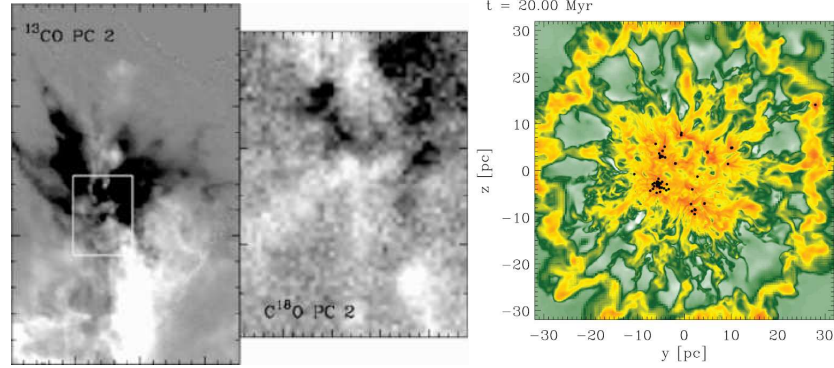


Fig. 6 *Left and middle panels:* Second eigenimages obtained by Principal Component Analysis of spectroscopic data of the star-forming region NGC 1333, showing the main contribution to the linewidth of molecular emission in this region (Brunt et al., 2009). The middle image shows the region enclosed in the rectangle in the left image. Black and white colors represent oppositely-signed components of the velocity. Brunt et al. (2009) describe the pattern as a “dipole”, in which large-scale patches of alternating velocity direction are observed. This is seen in both the large-scale and the small-scale images. *Right panel:* Image of the projected density field of a 3D numerical simulation with cooling, self-gravity, and magnetic fields, representing the formation of a dense atomic cloud by the collision of WNM streams in the direction perpendicular to the plane of the figure. The time shown is 20 Myr after the start of the simulation. The black dots denote “sink” particles, which replace local collapsing zones in the simulation. The whole cloud is also collapsing, although its collapse is not completed yet by the end of the simulation, at $t = 31$ Myr. From Vázquez-Semadeni et al. (2011).

verging flows in the simulations of Vázquez-Semadeni et al. (2007) were observed to be small compared to the velocities that develop due to the subsequent gravitational contraction, while in the simulations of (Banerjee et al., 2009), the clumps with highest internal velocity dispersions were those that had already formed collapsed objects (“sink” particles), although energy feedback from the sinks was not included.

All of the above evidence suggests that the observed supersonic motions in molecular clouds may have a significant, perhaps dominant, component of infalling motions, with a (possibly subdominant) superposed random (turbulent) component remaining from the initial stages of the cloud (Bate et al., 2003; Ballesteros-Paredes et al., 2011a,b), and perhaps somewhat amplified by the collapse (Vázquez-Semadeni et al., 1998). In this scenario of *hierarchical gravitational fragmentation*, the first structures that complete their collapse are small-scale, high-amplitude density fluctuations that are embedded within larger-scale, smaller amplitude ones, which complete their collapse later (Vázquez-Semadeni et al., 2009). The main role of the truly turbulent (i.e., fully random) motions is to provide the nonlinear density fluctuation seeds that will collapse locally after the global contraction increases their density sufficiently for them to become locally gravitationally unstable (Clark & Bonnell,

2005). Evidence for such multi-scale collapse has recently begun to be observationally detected (Galván-Madrid et al., 2009; Schneider et al., 2010).

7 Summary and Conclusions

In this contribution, we have briefly reviewed the role of two fundamental physical processes (net radiative cooling and self-gravity) that shape the nature of interstellar turbulence. We first discussed the effects of the net thermal effects that arise from several microphysical processes in the ISM, such as the emission of radiation from various ions, atoms, and molecules, which carries away thermal energy previously stored in the particles by collisional excitation, thus cooling the gas, and photo-electric production of energetic electrons off dust grains by background stellar UV radiation, which heats the gas. The presence of radiative heating and cooling implies in general that the gas behaves in a non-isentropic (or non-adiabatic) way, and in particular it may become *thermally unstable* in certain regimes of density and temperature, where small (i.e., *linear*) perturbations can cause runaway heating or cooling of the gas that only stops when the gas exits that particular regime. This in turn causes the gas to avoid those unstable density and temperature ranges, and tend to settle in the stable ones, thus tending to segregate the gas into different phases of different densities and/or temperatures. In classical models of the ISM, only the stable phases were expected to exist.

We then discussed the interaction between trans- or supersonic turbulence, which produces large (i.e., *nonlinear*) density and velocity, and thermal instability (TI). We first discussed the probability density function (PDF) of the density fluctuations, which takes a lognormal form in isothermal regimes, and develops power-law tails in polytropic (i.e., of the form $P \propto \rho^{\gamma_e}$) ones. We then noted that, since turbulence is an inherently mixing phenomenon, it opposes the segregating effect of thermal instability, causing the production of gas parcels in the classically forbidden unstable regimes, which may add up to nearly half the mass of the ISM, although the density PDF in general still exhibits some multimodality due to the gas' preference to settle in the stable regimes. The existence of gas in the unstable ranges has been confirmed by numerous observational studies.

We next discussed the nature of the turbulence in the different ranges of density and temperature of the gas, noting that in the diffuse ionized regions, where the flow is transonic (i.e., with Mach numbers $M_s \sim 1$), the gas appears to behave in an essentially incompressible way, exhibiting Kolmogorov scalings over many orders of magnitude in length scale. However, in the neutral atomic regions, where the gas is expected to be thermally unstable under the so-called *isobaric criterion*, the flow is expected to exhibit large density and temperature fluctuations, by up to factors ~ 100 , thus being highly fragmented. Numerical simulations of this process suggest that the gas is transonic with respect to the warm diffuse component, but supersonic with respect to the cold, dense one, although those supersonic motions appear to correspond more to the velocity dispersion of the dense clumps within

the warm substrate, rather than to the internal velocity dispersion within the clumps themselves.

Finally, we pointed out that large-scale compressions in the warm neutral gas, which may be triggered by either random turbulent motions, or by yet larger-scale instabilities, may nonlinearly induce the formation of large regions of dense, cold gas; much larger, in particular, than the most unstable scales of TI, which have sizes ~ 0.1 pc. These large clouds may easily be large enough to be *gravitationally* unstable, and numerical simulations of their evolution suggest that they rapidly engage in gravitational contraction. The latter may in fact promote the formation of molecules, so that the clouds are likely to become molecular only after they begin contracting. In addition, the clouds are born internally turbulent by the combined effect of TI and other dynamical instabilities, and the resulting nonlinear density fluctuations (“clumps”) may themselves become locally gravitationally unstable during the contraction of the whole large-scale cloud. Because they are denser, they have shorter free-fall times, and can complete their local collapses before the global one does, thus producing a regime of *hierarchical gravitational fragmentation*, with small-scale, short-timescale collapses occurring within larger-scale, longer-timescale ones. It is thus quite likely that the flow regime in the dense molecular clouds corresponds to a dominant multi-scale gravitational contraction, with smaller-amplitude random (“turbulent”) motions superposed on it. Interstellar turbulence is seen to involve an extremely rich and complex phenomenology, even more so than the already-fascinating regimes of terrestrial turbulence.

References

- Armstrong, J. W., Rickett, B. J., & Spangler, S. R. 1995, *ApJ*, 443, 209
- Audit, E., & Hennebelle, P. 2005, *A&A*, 433, 1
- Ballesteros-Paredes, J., Hartmann, L. W., Vázquez-Semadeni, E., Heitsch, F., & Zamora-Avilés, M. A. 2011, *MNRAS*, 411, 65
- Ballesteros-Paredes, J., Vázquez-Semadeni, E., Gazol, A., et al. 2011, *MNRAS*, 416, 1436
- Banerjee, R., Vázquez-Semadeni, E., Hennebelle, P., & Klessen, R. S. 2009, *MNRAS*, 398, 1082
- Bate, M. R., Bonnell, I. A., & Bromm, V. 2003, *MNRAS*, 339, 577
- Bergin, E. A., Hartmann, L. W., Raymond, J. C., & Ballesteros-Paredes, J. 2004, *ApJ*, 612, 921
- Blaisdell, G. A., Mansour, N. N., & Reynolds, W. C. 1993, *J. Fluid Mech.*, 256, 443
- Blandford, R., & Eichler, D. 1987, *Phys. Rep.*, 154, 1
- Blitz, L., & Shu, F. H. 1980, *ApJ*, 238, 148
- Brunt, C. M., Heyer, M. H., & Mac Low, M. 2009, *A&A*, 504, 883
- Burgers, J. M. 1974, “The nonlinear Diffusion Equation”, Reidel, Dordrecht
- Chepurnov, A., & Lazarian, A. 2010, *ApJ*, 710, 853
- Cho, J., Lazarian, A., & Vishniac, E. T. 2003, *Turbulence and Magnetic Fields in Astrophysics*, 614, 56
- Clark, P. C., & Bonnell, I. A. 2005, *MNRAS*, 361, 2
- Cox, A. N. 2000, *Allen’s Astrophysical Quantities*, Springer. Edited by Arthur N. Cox. ISBN: 0387987460
- Dalgarno, A., & McCray, R. A. 1972, *ARAA*, 10, 375
- de Avillez, M. A., & Breitschwerdt, D. 2005, *A&A*, 436, 585
- Dickey, J. M., Terzian, Y., & Salpeter, E. E. 1978, *ApJS*, 36, 77

- Elmegreen, B. G. 1991, NATO ASIC Proc. 342: The Physics of Star Formation and Early Stellar Evolution, 35
- Elmegreen, B. G., & Scalo, J. 2004, ARAA, 42, 211
- Federrath, C., Klessen, R. S., & Schmidt, W. 2008, ApJL, 688, L79
- Ferrière, K. M. 2001, Reviews of Modern Physics, 73, 1031
- Field, G. B. 1965, ApJ, 142, 531
- Field, G. B., Goldsmith, D. W., & Habing, H. J. 1969, ApJL, 155, L149
- Galván-Madrid, R., Keto, E., Zhang, Q., et al. 2009, ApJ, 706, 1036
- Gazol, A., Vázquez-Semadeni, E., Sánchez-Salcedo, F. J., & Scalo, J. 2001, ApJL, 557, L121
- Gazol, A., Vázquez-Semadeni, E., & Kim, J. 2005, ApJ, 630, 911
- Glover, S. C. O., & Mac Low, M.-M. 2007, ApJ, 659, 1317
- Goldreich, P., & Kwan, J. 1974, ApJ 189, 441
- Goldreich, P., & Sridhar, S. 1995, ApJ, 438, 763
- Hartmann, L., Ballesteros-Paredes, J., & Bergin, E. A. 2001, ApJ, 562, 852
- Heiles, C. 2001, ApJL, 551, L105
- Heiles, C. & Troland, T. H. 2003, ApJ, 586, 1067
- Heitsch, F., Burkert, A., Hartmann, L. W., Slyz, A. D., & Devriendt, J. E. G. 2005, ApJL, 633, L113
- Heitsch, F., & Hartmann, L. 2008, ApJ, 689, 290
- Heitsch, F., Hartmann, L. W., & Burkert, A. 2008, ApJ, 683, 786
- Heitsch, F., Hartmann, L. W., Slyz, A. D., Devriendt, J. E. G., & Burkert, A. 2008, ApJ, 674, 316
- Hennebelle, P., & Audit, E. 2007, A&A, 465, 431
- Hennebelle, P., Banerjee, R., Vázquez-Semadeni, E., Klessen, R.S., & Audit, E. 2008, A&A, 486, L43
- Hennebelle, P., & Péroult, M. 1999, A&A, 351, 309
- Heyer, M. H., & Brunt, C. M. 2004, ApJL, 615, L45
- Koyama, H., & Inutsuka, S.-I. 2000, ApJ, 532, 980
- Koyama, H., & Inutsuka, S.-i. 2002, ApJL, 564, L97
- Kritsuk, A. G., & Norman, M. L. 2002, ApJL, 569, L127
- Kwan, J. 1979, ApJ, 229, 567
- Landau, L. D., & Lifshitz, E. M. 1959, Course of theoretical physics. Fluid Mechanics, Oxford: Pergamon Press.
- Larson, R. B. 1981, MNRAS, 194, 809
- Mac Low, M.-M., Klessen, R. S., Burkert, A., & Smith, M. D. 1998, Physical Review Letters, 80, 2754
- Mac Low, M.-M., Balsara, D. S., Kim, J., & de Avillez, M. A. 2005, ApJ, 626, 864
- Mac Low, M.-M., & Klessen, R. S. 2004, Reviews of Modern Physics, 76, 125
- McKee, C. F. 1989, ApJ, 345, 782
- McKee, C. F., & Ostriker, J. P. 1977, ApJ, 218, 148
- McKee, C. F., & Ostriker, E. C. 2007, ARAA, 45, 565
- Meerson, B. 1996, Reviews of Modern Physics, 68, 215
- Myers, P. C. 1978, ApJ, 225, 380
- Norman, C., & Silk, J. 1980, ApJ, 238, 158
- Osterbrock, D. E., & Ferland, G. J. 2006, Astrophysics of gaseous nebulae and active galactic nuclei, 2nd. ed. by D.E. Osterbrock and G.J. Ferland. Sausalito, CA: University Science Books, 2006,
- Padoan, P., & Nordlund, Å. 1999, ApJ, 526, 279
- Padoan, P., Nordlund, A., & Jones, B. J. T. 1997, MNRAS, 288, 145
- Passot, T., & Vázquez-Semadeni, E. 1998, Phys. Rev. E, 58, 4501
- Passot, T., Vázquez-Semadeni, E., & Pouquet, A. 1995, ApJ, 455, 536
- Piontek, R. A., & Ostriker, E. C. 2004, ApJ, 601, 905
- Piontek, R. A., & Ostriker, E. C. 2005, ApJ, 629, 849
- Sánchez-Salcedo, F. J., Vázquez-Semadeni, E., & Gazol, A. 2002, ApJ, 577, 768
- Schneider, N., Bontemps, S., Simon, R., et al. 2011, A&A, 529, A1

- Schneider, N., Csengeri, T., Bontemps, S., et al. 2010, *A&A*, 520, A49
- Shu, F. H. 1992, *Physics of Astrophysics*, Vol. II, by Frank H. Shu. Published by University Science Books
- Shu, F. H., Adams, F. C., & Lizano, S. 1987, *ARAA*, 25, 23
- Stone, J. M., Ostriker, E. C., & Gammie, C. F. 1998, *ApJL*, 508, L99
- Sutherland, R. S., & Dopita, M. A. 1993, *ApJS*, 88, 253
- Toalá, J. A., Vázquez-Semadeni, E., & Gómez, G. C. 2012, *ApJ*, 744, 190
- Vázquez-Semadeni, E. 1994, *ApJ*, 423, 681
- Vázquez-Semadeni, E. 1999, *Millimeter-Wave Astronomy: Molecular Chemistry & Physics in Space*, 241, 161
- Vázquez-Semadeni, E., Banerjee, R., Gómez, G. C., et al. 2011, *MNRAS*, 414, 2511
- Vázquez-Semadeni, E., Cantó, J., & Lizano, S. 1998, *ApJ*, 492, 596
- Vázquez-Semadeni, E., Colín, P., Gómez, G. C., Ballesteros-Paredes, J., & Watson, A. W. 2010, *ApJ*, 715, 1302
- Vázquez-Semadeni, E., Gazol, A., & Scalo, J. 2000, *ApJ*, 540, 271
- Vázquez-Semadeni, E., Gazol, A., Passot, T., & et al. 2003, in “Turbulence and Magnetic Fields in Astrophysics”, *Lecture Notes in Physics*, 614, 213
- Vázquez-Semadeni, E., Gómez, G. C., Jappsen, A. K., et al. 2007, *ApJ*, 657, 870
- Vázquez-Semadeni, E., Gómez, G. C., Jappsen, A.-K., Ballesteros-Paredes, J., & Klessen, R. S. 2009, *ApJ*, 707, 1023
- Vázquez-Semadeni, E., González, R. F., Ballesteros-Paredes, J., Gazol, A., & Kim, J. 2008, *MNRAS*, 390, 769
- Vázquez-Semadeni, E., Ostriker, E. C., Passot, T., Gammie, C. F., & Stone, J. M. 2000, *Protostars and Planets IV*, 3
- Vázquez-Semadeni, E., Passot, T., & Pouquet, A. 1996, *ApJ*, 473, 881 (VPP96)
- Vázquez-Semadeni, E., Ryu, D., Passot, T., González, R. F., & Gazol, A. 2006, *ApJ*, 643, 245
- Vishniac, E. T. 1994, *ApJ*, 428, 186
- Walder, R., & Folini, D. 2000, *ApSS*, 274, 343
- Williams, J. P., de Geus, E. J., & Blitz, L. 1994, *ApJ*, 428, 693
- Wolfire, M. G., Hollenbach, D., McKee, C. F., Tielens, A. G. G. M., & Bakes, E. L. O. 1995, *ApJ*, 443, 152
- Zuckerman, B., & Evans, N. J. 1974, *ApJ*, 192, L149
- Zuckerman, B. & Palmer, P. 1974, *ARA&A*, 12, 279